

Article

Highly Sulfonated Diamine Synthesized Polyimides and Protic Ionic Liquid Composite Membranes Improve PEM Conductivity

Bor-Kuan Chen ^{1,*}, Tzi-Yi Wu ², Jhong-Ming Wong ¹, Yu-Ming Chang ¹, Hsu-Feng Lee ³, Wen-Yao Huang ³ and Antonia F. Chen ⁴

¹ Department of Materials Engineering, Kun Shan University, Tainan 710, Taiwan; E-Mails: sako_wan@hotmail.com (J.-M.W.); lost0726@hotmail.com (Y.-M.C.)

² Department of Chemical and Materials Engineering, National Yunlin University of Science and Technology, Yunlin 640, Taiwan; E-Mail: wuty@yuntech.edu.tw

³ Institute of Electro-Optical Engineering, National Sun Yat-sen University, Kaohsiung 804, Taiwan; E-Mails: 14013010114abc@yahoo.com.tw (H.-F.L.); wyhuang@faculty.nsysu.edu.tw (W.-Y.H.)

⁴ Department of Orthopaedic Surgery, Rothman Institute, Philadelphia, PA 19107, USA; E-Mail: antoniachen@rothmaninstitute.com

* Author to whom correspondence should be addressed; E-Mail: chenbk@mail.ksu.edu.tw; Tel.: +886-6205-1253; Fax: +886-6205-0493.

Academic Editor: Scott M. Husson

Received: 17 April 2015 / Accepted: 28 May 2015 / Published: 8 June 2015

Abstract: A novel sulfonated diamine was synthesized from 1,4-bis(4-aminophenoxy) benzene [*p*BAB]. Sulfonated polyimides (SPIs) were synthesized from sulfonated *p*BAB, 1,4-bis(4-aminophenoxy-2-sulfonic acid) benzenesulfonic acid [*p*BABTS], various diamines and aromatic dianhydrides. Composite proton exchange membranes (PEMs) made of novel SPIs and a protic ionic liquid (PIL) 1-vinyl-3-*H*-imidazolium trifluoromethanesulfonate [VIm][OTf] showed substantially increased conductivity. We prepared an SPI/PIL composite PEM using *p*BABTS, 4,4'-(9-fluorenylidene) dianiline (9FDA) as diamine, 3,3',4,4'-diphenylsulfone tetracarboxylic dianhydride (DSDA) as dianhydride and 40 wt % [VIm][OTf] with a high conductivity of 16 mS/cm at 120 °C and anhydrous condition. *p*BABTS offered better conductivity, since the chemical structure had more sulfonated groups that provide increased conductivity. The new composite membrane could be a promising anhydrous or low-humidity PEM for intermediate or high-temperature fuel cells.

Keywords: proton exchange membrane; sulfonated diamine; sulfonated polyimide; ionic liquid; conductivity

1. Introduction

The proton exchange membrane (PEM), a crucial component of proton exchange membrane fuel cells (PEMFCs), serves as a medium for conducting protons from the anode to the cathode, acts as a separator of gaseous reactants, and determines the efficiency of PEMFCs [1]. A PEMFC directly converts the chemical energy of hydrogen and oxygen into electrical energy. PEMFCs have been shown to exhibit effective and high-energy conversion, high proton conductivities, and excellent energy density, and have therefore become an attractive power source for automotive, stationary, and mobile power applications [2]. Perfluorosulphonic acid-based membranes such as Nafion[®] (DuPont) have been widely used for the polymer electrolytes of PEMFCs. Nafion PEM has elicited great interest because it exhibits high combined chemical, electrochemical, and mechanical stability with high proton conductivity at ambient temperatures. However, Nafion PEM is associated with high costs, serious methanol crossover, and loss of conductivity at temperatures higher than 80 °C and at low relative humidity [3]. Therefore, the development of alternative PEMs that are more cost-effective than perfluorinated ionomers and can be employed over a wider temperature range with high proton conductivity have been extensively studied as polymer electrolytes for PEMFCs [3,4].

Sulfonated aromatic hydrocarbon polymers have attracted considerable attention because of their excellent thermal and mechanical stabilities. High degrees of sulfonation can provide sulfonated aromatic hydrocarbon polymers with high proton conductivity and offer great potential as PEMs for fuel cell applications [4]. Of the many advanced sulfonated polymers such as poly(ether ketone), poly(ether ether ketone) (PEEK), polybenzimidazole (PBI), and polyimide (PI), sulfonated aromatic PIs are considered one of the most promising PEMs to be used in fuel cells [5,6]. These materials exhibit most of the required properties for PEM application, including a high level of ionic conductivity, low methanol permeability, and good mechanical properties. The main synthesis route for sulfonated polyimides (SPIs) is direct polymerization using sulfonated diamine monomers by reacting with aromatic dianhydride via chemical imidization through poly(amic acid) (PAA) [7].

There are significant economic and technological advantages for operating a PEMFC at temperatures above 100–150 °C, including co-generation of heat and power, high tolerance to fuel impurities, and a simpler system design [1]. PEM is one of the key components in the development of intermediate- to high-temperature PEMFCs. The PEM not only needs to be highly stable in the harsh environment of fuel cells, but must also possess high proton conductivity at elevated temperatures under low humidity. Great efforts have been made to develop intermediate or elevated temperature PEMs [1,4,5,8]. The temperature range of 80–130 °C is within the domain of many novel materials. Sulfonated hydrocarbon-based membranes and inorganic composite membranes have been explored, along with the application of ionic liquid (IL) doped into hydrocarbon-based membranes, to promote the performance of PEM above 100 °C [3,8–14]. ILs are molten salts that have attracted much attention in recent years because of their exceptional properties, including negligible vapor pressure,

inflammability, high thermal and electrochemical stability, and outstanding ionic conductivity even under anhydrous conditions [15,16]. One significant advantage to using ILs as the proton transporting medium in the membrane is that ionic conductivity at elevated temperatures is less humidity-dependent [8]. Protic ILs (PILs) have even higher ionic conductivity than common ILs (which are usually aprotic), and most importantly, PILs are desired due to their intrinsic proton conductivity [17]. PILs can transfer protons from acid to base, leading to the presence of proton donor and acceptor sites that can be used to build a hydrogen-bonded network [18]. Conrad and Vankelecom have studied imidazolium methanesulfonate as a proton conductor for high-temperature PEMFCs [9]. The continuing improvements in PIL-based PEMs have led to many attractive results in a growing number of research studies [8,9,12–14,17–21]. Various PILs have also been applied in SPI PEMs. Watanabe *et al.* [12] used the PIL diethylmethyl ammonium trifluoromethanesulfonate [dema][OTf], which functions as a proton conductor. Polymer electrolyte membranes for non-humidified fuel cells were prepared by the solvent casting method using SPI and [dema][OTf]. The composite membranes had good thermal stability and ionic conductivity ($>10^{-2}$ S cm⁻¹ at 120 °C) under anhydrous conditions. Deligöz and Yılmazoğlu [19] prepared SPI/IL composite membranes with high ionic conductivity by utilizing IL *N*-methyl imidazolium tetrafluoroborate doped into a SPI which was synthesized from 2,4-diaminobenzene sulfonic acid and reacted with benzophenon-tetracarboxylic dianhydride. Borneman *et al.* proposed the use of IL 1-*H*-3-methylimidazolium bis(trifluoromethanesulfonyl) imide as a conductive filler in a tailor-made porous PBI support as a PEM for high-temperature fuel cell applications [21]. These types of composite membranes possessed good thermal stability and high ionic conductivity, but were usually accompanied by reduced mechanical strength and dimensional stability, especially at elevated temperatures. Increasing the polymer content leads to the improvement of mechanical properties, but is accompanied by a reduction in ionic conductivity [8]. Hwang *et al.* [22] used only 0.5 wt % loading of graphene-modified PIL-based composite membrane as a PEM that exhibited dramatic enhancements in ionic conductivity and mechanical properties. The research on high conductivity PEMs prepared by sulfonated polymers modified with PILs is growing, since there are a large number of combinations of polymer and PIL. The benefit of SPI doped with PIL is that the ionic interaction between sulfonic acid groups and PIL cation (imidazolium groups) provides structural reinforcement of the polymer matrix at high temperatures, and also limits IL migration resulting in long-term conductivity stability [19].

In recent years, we have synthesized and characterized several polyimides and investigated a series of novel ionic liquids. We attempted to improve the conductivity of PEMs by utilizing a sulfonated diamine, 4,4'-diamino diphenylether-2,2'-disulfonic acid (ODADS) to synthesize SPIs that were doped with a PIL 1-vinyl-3-*H*-imidazolium trifluoromethanesulfonate [VIm][OTf] to fabricate composite membranes [13,14]. We prepared SPI/PIL composite PEM using 50 wt % [VIm][OTf] with a high conductivity of 7 mS/cm at 100–120 °C and anhydrous condition depending on the ODADS content and dianhydride [14]. To further improve the conductivity of composite PEMs in this study, we first synthesized a novel sulfonated diamine 1,4-bis(4-aminophenoxy-2-sulfonic acid) benzenesulfonic acid [*p*BABTS], and fabricated high-conductivity composite PEMs using *p*BABTS synthesized SPIs as a matrix polymer that were doped with the PIL [VIm][OTf] 40%. A high conductivity of 16 mS/cm at 120 °C and anhydrous condition was achieved. We also studied the effect of various diamines on the conductivity of PEMs made from *p*BABTS. Three diamines were used: 2,2-bis[4-(4-amino-phenoxy) phenyl] propane (BAPP), 2,7-bis(4-aminophenoxy) naphthalene (BAPN), and 4,4'-(9-fluorenylidene)

dianiline (9FDA). The impact of aromatic dianhydride on the conductivity of SPI/PIL PEMs was noted in our recent study [14]. Three aromatic dianhydrides were investigated: 4,4'-oxydiphthalic anhydride (ODPA), naphthalene-1,4,5,8-tetracarboxylic dianhydride (NTDA), and 3,3',4,4'-diphenyl sulfone tetracarboxylic dianhydride (DSDA). We investigated the electrochemical and thermal properties of these SPI/PIL composite membranes. The aim of this work was to utilize a novel highly sulfonated diamine *p*BABTS and various combinations of diamine and dianhydride to prepare SPI/PIL composite membranes to substantially increase the conductivity of PEMs for installation into hydrogen/oxygen fuel cells.

2. Experimental Section

2.1. Materials

Chemicals of reagent grade were purchased from various commercial sources. We obtained hydroquinone, 4-chloronitrobenzene, 2,7-dihydroxynaphthalene, and 1-methoxypropan-2-ol from Acros Organics (Geel, Belgium); and *m*-cresol, concentrated sulfuric acid, fuming sulfuric acid (SO₃, 20%), potassium carbonate, hydrazine monohydrate, and 10% palladium on activated carbon were obtained from Sigma-Aldrich (St. Louis, MO, USA) and used as received without further purification. Diamines, 2,2-bis[4-(4-amino-phenoxy)phenyl]propane (BAPP), and 9,9-bis(4-aminophenyl)fluorene (9FDA) were purchased from Tokyo Chemical Industry (TCI) (Tokyo, Japan). 2,7-bis(4-aminophenoxy) naphthalene (BAPN) was prepared according to a procedure described in the literature [23]. Dianhydrides, 4,4'-oxydiphthalic anhydride (ODPA), and naphthalene-1,4,5,8-tetracarboxylic dianhydride (NTDA) were obtained from Aldrich, and 3,3',4,4'-diphenylsulfone tetracarboxylic dianhydride (DSDA) was purchased from TCI. All dianhydrides were used after thermal treatment in a vacuum at 150 °C to cyclize possible impurities. PIL, 1-vinyl-3-*H*-imidazolium trifluoromethanesulfonate [VIm][OTf] was prepared according to our previous report [13]. The chemical structure of [VIm][OTf] is shown in Figure 1. Nafion 117 membranes as the reference membrane were acquired from Du Pont Co. (Wilmington, DE, USA).

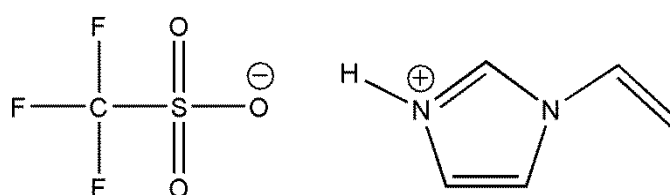


Figure 1. Chemical structures of PIL [VIm][OTf].

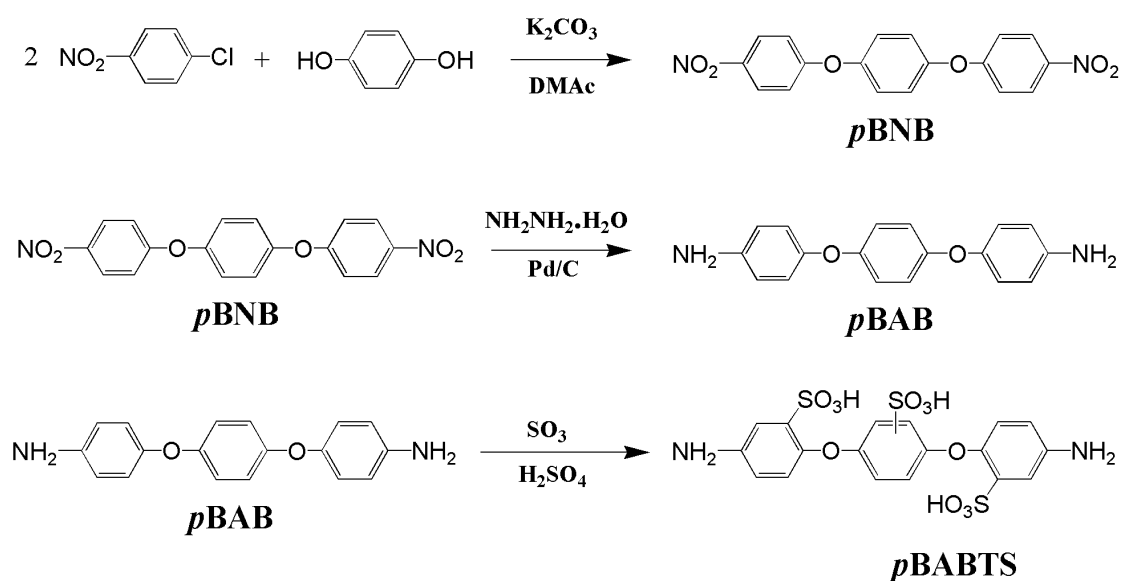
2.2. Synthesis of 1,4-Bis(4-aminophenoxy-2-sulfonic acid) Benzenesulfonic Acid (*p*BABTS)

The title compound was synthesized in three steps. In the first step, a mixture of 10.00 g (0.09 mol) of hydroquinone, 25.0 g (0.18 mol) of anhydrous K₂CO₃, and 28.4 g (0.18 mol) of 4-chloronitrobenzene was charged into a 500 mL four-neck round bottom flask that contained 350 mL of dimethyl acetamide (Scheme 1). The flask was heated at 373 K for 20 h under a nitrogen atmosphere. The color of the solution changed from yellow to dark brown as the reaction proceeded. After cooling to room

temperature, the reaction mixture was poured in 2000 mL of water to precipitate a yellow solid, which was washed thoroughly with water and then separated by filtration. The resulting crude solid was recrystallized from 250 mL of 1-methoxypropan-2-ol and dried at 100 °C in vacuo to obtain 1,4-bis(4-nitrophenoxy)benzene [*p*BNB] (yield 87%, m.p. 244 °C).

In the second step, a 500 mL four-neck flask was charged with 40.0g (0.1136 mol) of *p*BNB, 70 mL of hydrazine monohydrate, 330 mL of ethanol, and 1.2 g of 10% palladium on carbon (Pd/C). The mixture was refluxed for 20 h and then filtered to remove Pd/C. The solvent was evaporated and the resulting crude solid was recrystallized from ethanol to create 1,4-bis(4-aminophenoxy)benzene [*p*BAB] crystals (yield 85%, m.p. 174 °C).

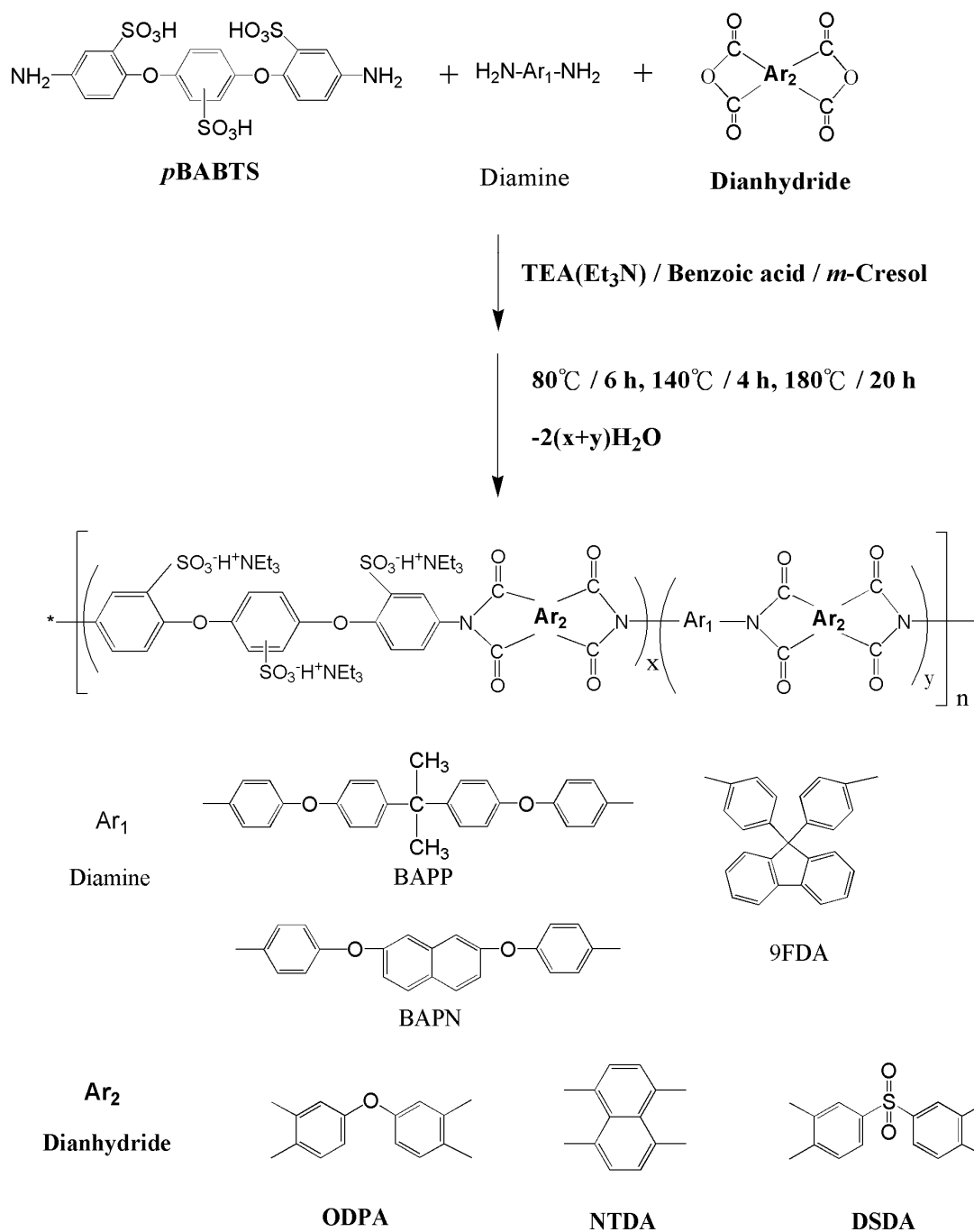
The last step was the sulfonation of *p*BAB. A 250 mL three-neck flask under a nitrogen atmosphere equipped with a mechanical stirring device was charged with 14.612 g (50 mmol) of *p*BAB. The flask was cooled in an ice bath, and 8.5 mL of concentrated sulfuric acid was slowly added while stirring the mixture. After *p*BAB was completely dissolved, 46.8 mL of fuming sulfuric acid (SO₃, 20%) was slowly added to the flask. The reaction mixture was stirred at 0 °C for 2 h and then slowly heated to 80 °C and kept at this temperature for 4 h. After cooling to room temperature, the slurry was carefully poured into 150 g of crushed ice. The resulting white precipitate was filtered off and then re-dissolved in a 10% sodium hydroxide solution. The basic solution was filtered, and the filtrate was acidified with concentrated hydrochloric acid. The solid was filtered off, washed with water and methanol successively, and dried at 80 °C in vacuo. White product *p*BABTS was obtained with a yield of 85%.



Scheme 1. Reaction scheme of sulfonated 1,4-bis(4-aminophenoxy)benzene.

2.3. Synthesis of Sulfonated Polyimides

Sulfonated PIs were synthesized by reacting diamines with dianhydride *via* chemical imidization through poly(amic acid) (PAA). A representative SPI (*p*BABTS/9FDA/DSDA with a molar ratio of 30/20/50) was prepared as follows:



Scheme 2. Reaction scheme of novel sulfonated polyimides.

In a 3-necked 250-mL round-bottom flask equipped with a nitrogen inlet/outlet, vapor trap, and stir motor, *p*BABTS (3.63 g, 6.82 mmol), triethylamine (TEA) (2.24 g, 22.1 mmol), and *m*-cresol (25 mL) were charged. The mixture was heated at 40 °C until the *p*BABTS was dissolved (about 1.5 h). 9FDA (1.585 g, 4.55 mmol), DSDA (4.07 g, 11.37 mmol), benzoic acid (2.38g, 19.5 mmol), and *m*-cresol (25 mL) were added to the agitated flask, the temperature was increased to 80 °C, and the mixture was stirred for 6 h. After the addition of toluene (50 mL), the temperature was raised to 140 °C and held for 4–6 h to complete azeotropic distillation. Then, the temperature was further increased to 180 °C and held for another 20 h. The reaction mass was cooled to room temperature before pouring it into 500 g acetone. After blending for 1 h, the mixture was filtered, and the solid was Soxhlet-extracted with

acetone overnight. Then the solid was vacuum dried at 120 °C for 24 h. See Scheme 2 for the reaction scheme and the chemical structures of the monomers used.

The code of materials and the amount of *p*BABTS, diamines, and dianhydrides used for various SPIs are listed in Table 1.

Table 1. The codes, mole fractions in feed and IEC of various sulfonated polyimides.

Code	Diamines Mole in Feed (mmol)		Dianhydride † (11.38 mmol)	IEC ^a (theory) (mmol/g)	IEC ^b (exp) (mmol/g)
	<i>p</i> BABTS	Diamine *			
SPI1pO	5.69	BAPP 5.69	ODPA	2.01	1.64
SPI2pO	6.83	BAPP 4.55	ODPA	2.38	1.97
SPI3pO	7.97	BAPP 3.41	ODPA	2.73	2.60
SPI1nO	5.69	BAPN 5.69	ODPA	2.11	1.60
SPI2nO	6.83	BAPN 4.55	ODPA	2.47	1.90
SPI3nO	7.97	BAPN 3.41	ODPA	2.80	2.40
SPI1fO	5.69	9FDA 5.69	ODPA	2.10	1.65
SPI2fO	6.83	9FDA 4.55	ODPA	2.46	1.98
SPI3fO	7.97	9FDA 3.41	ODPA	2.80	2.30
SPI1nN	5.69	BAPN 5.69	NTDA	2.24	1.72
SPI2nN	6.83	BAPN 4.55	NTDA	2.62	2.06
SPI3nN	7.97	BAPN 3.41	NTDA	2.97	2.38
SPI1nS	5.69	BAPN 5.69	DSDA	1.98	1.44
SPI2nS	6.83	BAPN 4.55	DSDA	2.31	1.68
SPI3nS	7.97	BAPN 3.41	DSDA	2.64	1.95
SPI1fS	5.69	9FDA 5.69	DSDA	1.97	1.44
SPI2fS	6.83	9FDA 4.55	DSDA	2.31	1.67
SPI3fS	7.97	9FDA 3.41	DSDA	2.63	1.84

* Diamine: *f* = 9FDA, *n* = BAPN, *p* = BAPP; † Dianhydride: *O* = ODPA, *N* = NTDA, *S* = DSDA;

^a IEC_(theory) was calculated from feed monomer ratios; ^b IEC_(exp) was measured by titration.

2.4. Preparation of SPI/PIL Composite Membranes

The composite membranes were fabricated using a solution casting method. SPI was first dissolved in *m*-cresol and appropriate amounts of [VIm][OTf] were added to a sealed sample bottle. The mixture was ultrasonicated for 6–8 h at room temperature to mix it completely, and was then cast on a Petri dish. Evaporation of *m*-cresol at 60 °C gave a uniform composite membrane. The composite membranes were peeled from the dish, dried in a vacuum oven at 120 °C overnight, and then cooled to room temperature. SPI/PIL composite membrane films were stored in an inert atmosphere glovebox. Table 2 lists codes and weight compositions of sulfonated polyimide/protic ionic liquid (SPI/PIL) composite films.

Table 2. Codes and weight compositions of sulfonated polyimide/protic ionic liquid (SPI/PIL) composite films.

Code	SPI	PIL *	Code	SPI	PIL *
SPI1pO/V ₄₀	SPI1pO 60%	VIm 40%	SPI1nN/V ₄₀	SPI1nN 60%	VIm 40%
SPI2pO/V ₄₀	SPI2pO 60%	VIm 40%	SPI2nN/V ₄₀	SPI2nN 60%	VIm 40%
SPI3pO/V ₄₀	SPI3pO 60%	VIm 40%	SPI3nN/V ₄₀	SPI3nN 60%	VIm 40%
SPI1nO/V ₄₀	SPI1nO 60%	VIm 40%	SPI1nS/V ₄₀	SPI1nS 60%	VIm 40%
SPI2nO/V ₄₀	SPI2nO 60%	VIm 40%	SPI2nS/V ₄₀	SPI2nS 60%	VIm 40%
SPI3nO/V ₄₀	SPI3nO 60%	VIm 40%	SPI3nS/V ₄₀	SPI3nS 60%	VIm 40%
SPI1fO/V ₄₀	SPI1fO 60%	VIm 40%	SPI1fS/V ₄₀	SPI1fS 60%	VIm 40%
SPI2fO/V ₄₀	SPI2fO 60%	VIm 40%	SPI2fS/V ₄₀	SPI2fS 60%	VIm 40%
SPI3fO/V ₄₀	SPI3fO 60%	VIm 40%	SPI3fS/V ₄₀	SPI3fS 60%	VIm 40%
			SPI1fS/V ₃₀	SPI1fS 70%	VIm 30%
			SPI2fS/V ₃₀	SPI2fS 70%	VIm 30%
			SPI3fS/V ₃₀	SPI3fS 70%	VIm 30%

* VIm = [VIm]/[OTf].

2.5. Characterization

The chemical structures of compounds, SPI, and SPI/PIL were identified using Fourier transform infrared (FTIR) and ¹H nuclear magnetic resonance (NMR) spectroscopy. FTIR spectra were recorded on a Bio–Rad Digilab FTS-40 spectrometer (Bio–Rad, Cambridge, MA, USA). Both the transmission and the attenuated total reflectance (ATR) spectra were recorded at a resolution of 8 cm^{−1} and with an accumulation of 16 scans. ¹H NMR spectra were recorded on BRUKER AV300 and AV400 spectrometers (Billerica, MA, USA), respectively.

The ion exchange capacity (IEC) was measured by titration. Acidified SPI membranes were vacuum dried until constant weights were obtained. The membranes were then immersed in 50 mL of saturated NaCl solution for two days to exchange H⁺ with sodium ions. The liberated H⁺ ions were identified by titration with 0.01 N NaOH, and phenolphthalein was used as the indicator. The values of IEC were obtained using the following equation:

$$\text{IEC (mmol/g)} = [C_{\text{NaOH}}] V / W_{\text{membrane}} \quad (1)$$

where [C_{NaOH}] is the concentration of NaOH, *V* is the volume of NaOH consumed and *W*_{membrane} is the weight of dried membrane.

The ionic conductivity (σ) of the membranes was determined by AC impedance spectroscopy (CH Instruments, CHI 660B, Austin, TX, USA) under anhydrous or non-humid conditions. The membrane was sandwiched between two parallel stainless steel discs (φ = 1.0 cm). The frequency ranged from 100 kHz to 10 Hz at a perturbation voltage of 10 mV. The ionic conductivity was calculated from the electrolyte resistance (*R*) obtained from the intercept of the Nyquist plot with the real axis, the membrane thickness (*d*) and the electrode area (*A*) according to the equation:

$$\sigma = d / (A \cdot R) \quad (2)$$

The error in proton conductivity measurement, caused mainly by the deviation of cell temperature and thickness, was estimated to be less than 10%.

The morphologies of sulfonated PIs and SPI/PIL films were observed with a JEOL JSM-6700 scanning electron microscope (SEM) (Tokyo, Japan) with an accelerating voltage of 3–5 kV. An Oxford Instruments energy-dispersive X-ray spectrometer (EDS) was used to obtain the element mapping image and was recorded on the SEM.

The thermal properties of the materials were characterized by thermogravimetric analysis (TGA) and differential scanning calorimetry (DSC). TGA was performed with a Perkin–Elmer Pyris 1 TGA (Waltham, MA, USA) at a heating rate of 10 °C min⁻¹ in N₂. Each sample weight was about 5 mg. DSC data were obtained from a Perkin–Elmer Pyris Diamond DSC. Samples were scanned at a heating rate of 10 °C min⁻¹ under N₂. *T_g* (glass transition temperature) values were determined from the onset temperature of the change of the specific heat capacity in heat flow curves.

3. Results and Discussion

3.1. Sulfonation of *pBAB*

pBNB was prepared from hydroquinone and 4-chloronitrobenzene. The IR absorption band at 1345 cm⁻¹ was attributed to the –NO₂ group, which disappeared after the hydrogenation of *pBNB* to become *pBAB*. The absorption bands at 1634 cm⁻¹ and 3300–3500 cm⁻¹ were attributed to the –NH₂ group (Figure 2). *pBABTS* was prepared by direct sulfonation of the parent diamine *pBAB* using fuming sulfuric acid as the sulfonating agent. FTIR and ¹H NMR spectroscopy were used to confirm the presence of the pendant –SO₃H group on the monomer structure. Sulfonation of *pBAB* was confirmed by the presence of two sharp IR absorption bands at 1023 and 1086 cm⁻¹, which were due to the aromatic –SO₃H symmetric and asymmetric stretching vibrations, respectively. For sulfonated compounds, the degree of sulfonation was determined by the integration of some specific ¹H NMR peaks, which gave the ratio of sulfonated aromatic rings to unsubstituted *pBAB* [24]. From the ¹H NMR spectrum, the signals in range of 6.8–7.8 ppm are assigned to the aromatic protons in the ortho and meta positions of aromatic amino group, and para positions in benzene ring.

¹H NMR (500 MHz, DMSO-d₆): δ 9.77 (br, 3H, –SO₃H), 7.78 (d, 1H, Ar–H of –O–C–CH–CH–C–O–), 7.63 (d, 1H, Ar–H of –O–C–CH–CH–C–O–), 7.28 (s, 1H, –O–C–CH–C–SO₃H), 7.18–7.22 (m, 2H, Ar–H of H₂N–C–CH–CH–C–O–), 6.97 (d, 1H, Ar–H of H₂N–C–CH–C–SO₃H), 6.86 (d, 1H, Ar–H of H₂N–C–CH–C–SO₃H), 6.82 (d, 1H, Ar–H of H₂N–C–CH–CH–C–O–), 6.80 (d, 1H, Ar–H of H₂N–C–CH–CH–C–O–).

3.2. Synthesis of Sulfonated Polyimides

SPIs with various diamines and dianhydrides were synthesized. Figure 3 shows the FT-IR spectrum of SPI2fS. The intense absorption at 1730 and 1780 cm⁻¹ corresponds to C=O symmetric and asymmetric stretching, respectively, 1380 and 744 cm⁻¹ corresponds to C–N stretching and bending absorbance; at 1660 cm⁻¹ [C=O(CONH)] and 1550 cm⁻¹ (C–NH), no absorption bands were observed, which proves the success of imidization. The two sharp IR absorption bands at 1030 and 1086 cm⁻¹, which were a result of the aromatic –SO₃H symmetric and asymmetric stretching, confirmed the presence of –SO₃H in SPIs.

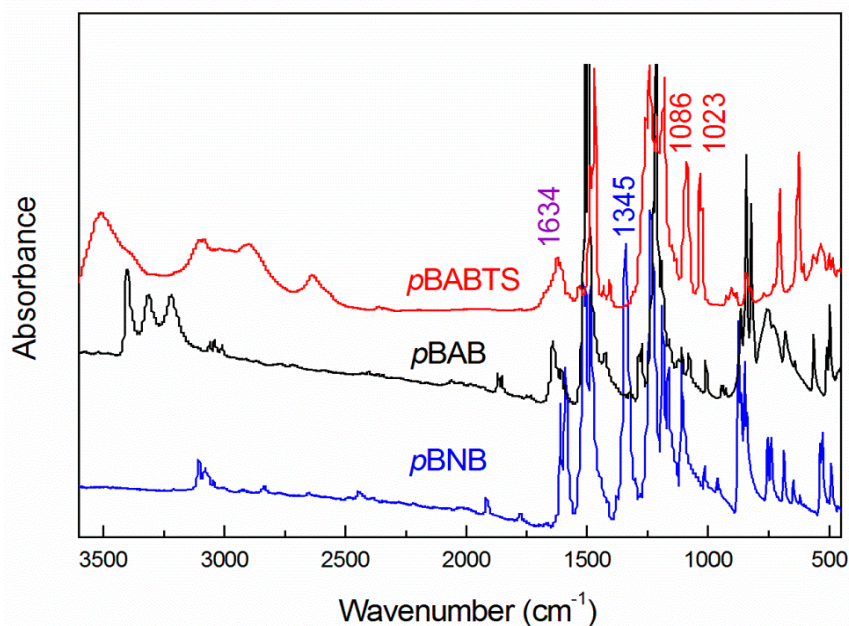


Figure 2. FTIR spectra of pBNB, pBAB and pBABTS.

3.3. Composite Membranes Structure Characterization

The composite SPI/PIL membranes were fabricated using the solution casting method with *m*-cresol as the casting solvent. The FTIR spectrum of a composite membrane is also shown in Figure 3. As expected, SPI/PIL composite membranes all had two sharp absorptions at 1030 and 1086 cm^{-1} , which resulted from the aromatic $-\text{SO}_3\text{H}$ symmetric and asymmetric stretching vibrations of SPI, respectively. The main absorptions at about 1780 and 1730 cm^{-1} were related to the asymmetric and symmetric stretching vibrations of imide $\text{C}=\text{O}$, and 1380 cm^{-1} corresponded to a $\text{C}-\text{N}$ stretching absorbance. The characteristic aromatic $\text{C}-\text{H}$ stretching of the imidazolium cation near 3160 cm^{-1} was detected [25]. The broadening of the bands in the region of 2400–3200 cm^{-1} was appertaining to the hydrogen bonding between $-\text{SO}_3^-$ of the anion and $-\text{NH}^+$ of the cation in [VIm][OTf] [25]. The absorption at 1660 cm^{-1} referred to the unique $\text{N}-\text{C}=\text{C}$ absorption of [VIm][OTf]. The absorption band at 1550 cm^{-1} was attributed to cationic $\text{C}=\text{N}$ in ionic liquid, and at 1260 and 640 cm^{-1} was from the absorption of $-\text{CF}_3$. The FTIR spectra further proved the formation of SPI/PIL composite membranes. All of the spectroscopic data obtained were consistent with the proposed chemical structures.

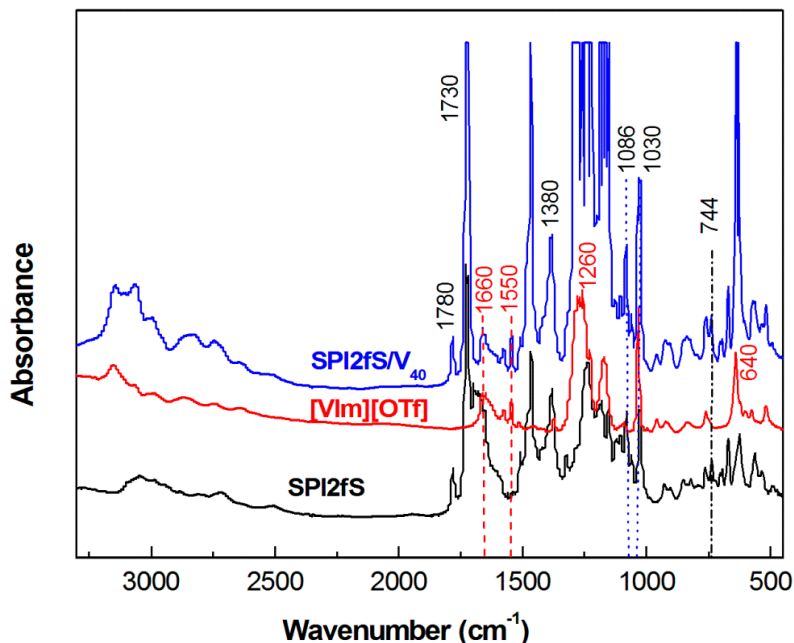


Figure 3. FTIR spectra of SPI2fS, [VIm][OTf], and its SPI/PIL composite film.

3.4. Thermal Properties

The thermal properties of the polymer materials were investigated using TGA and DSC under N_2 atmosphere. Table 3 lists the thermal decomposition temperatures at 10% weight loss ($T_{d-10\%}$) and glass transition temperatures (T_g). The thermal data indicated that the SPI/PIL composite films had high thermal stability. The TGA thermograms (shown in Figure 4) depict that there were several stages of weight loss for SPI. The first weight loss that occurred between 100 and 250 °C originated from the degradation of the attached sulfonic acid groups [14]. The second stage, which occurred between 300 and 380 °C, was attributable to the decomposition of the polyimide side chains. Finally, degradation occurred at temperatures higher than 450 °C that correspond to the pyrolysis of the SPI backbone. Table 3 shows that $T_{d-10\%}$ and T_g decreased with increasing amounts of *p*BABTS in SPIs, which indicated that *p*BABTS reduced thermal stability while softening SPIs. Since SPI membranes contained more sulfonic acid groups, they had more bonded water and decomposed easily [26]. Thermal data in Table 3 indicated that SPI doped with ionic liquid resulted in membranes that exhibited higher $T_{d-10\%}$ than pristine SPI polymers. Incorporation of [VIm][OTf] in the composite films affords almost no weight loss below 300 °C. This temperature was about the onset of degradation for the PIL used and it was still well above the operating temperature of a high temperature PEMFC (100–200 °C). The TGA data also showed that [VIm][OTf] had residues at high temperatures (Figure 4). This could account for the vinyl chemical structure of [VIm][OTf], which could be oligomerized or polymerized at 200 °C or higher temperatures [27]. As the thermal data indicated, T_g decreased with increasing amounts of *p*BABTS and PIL contents in SPI/IL composite membranes. Clearly, the T_g of SPI/PIL composite membranes decreased substantially compared with pristine SPI membranes. For practical purposes, the thermal data suggest that SPI/PIL composite membranes with T_g above 120 °C (the operating temperature of intermediate temperature PEMFC) could be employed as PEMs for fuel cell systems.

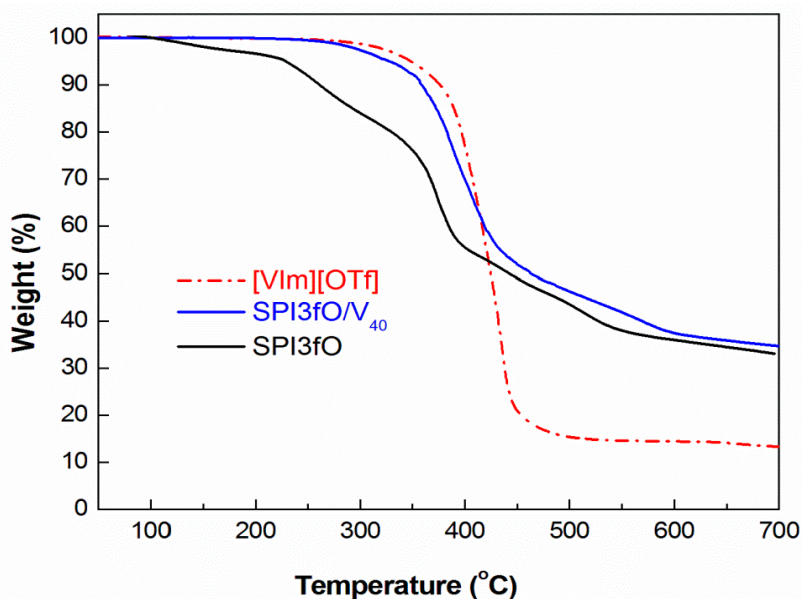


Figure 4. TGA scans of SPI, PIL and SPI/PIL composite membranes.

Table 3. Thermal properties of SPIs, PIL and SPI/PIL composite membranes.

Material	$T_{d-10\%}$ (°C)	T_g (°C)	Material	$T_{d-10\%}$ (°C)	T_g (°C)
SPI1pO	319.4	281.4	SPI1pO/V ₄₀	364.3	128.9
SPI2pO	295.0	235.2	SPI2pO/V ₄₀	358.7	112.0
SPI3pO	270.0	203.6	SPI3pO/V ₄₀	352.2	103.4
SPI1nO	329.5	319.0	SPI1nO/V ₄₀	355.4	139.4
SPI2nO	314.5	296.9	SPI2nO/V ₄₀	352.6	131.2
SPI3nO	295.2	281.7	SPI3nO/V ₄₀	341.3	118.2
SPI1fO	263.9	254.8	SPI1fO/V ₄₀	366.9	135.0
SPI2fO	254.0	245.2	SPI2fO/V ₄₀	358.6	126.2
SPI3fO	243.4	230.5	SPI3fO/V ₄₀	350.8	116.3
SPI1nN	334.3	301.7	SPI1nN/V ₄₀	353.9	160.3
SPI2nN	296.4	286.1	SPI2nN/V ₄₀	338.2	148.8
SPI3nN	271.5	260.2	SPI3nN/V ₄₀	312.8	128.5
SPI1nS	304.7	289.5	SPI1nS/V ₄₀	357.1	155.5
SPI2nS	275.8	260.4	SPI2nS/V ₄₀	343.2	146.6
SPI3nS	253.6	224.3	SPI3nS/V ₄₀	334.5	136.7
SPI1fS	282.1	247.5	SPI1fS/V ₄₀	358.7	137.5
SPI2fS	276.9	234.5	SPI2fS/V ₄₀	354.5	128.9
SPI3fS	233.7	224.7	SPI3fS/V ₄₀	345.6	100.3
			SPI1fS/V ₃₀	357.1	141.7
			SPI2fS/V ₃₀	347.4	132.4
			SPI3fS/V ₃₀	340.9	123.5
[VIm][OTf]	376.2	50.0			

3.5. Membrane Conductivity

Proton conductivity was generally thermally stimulated, and it was reasonable to observe an increase in conductivity with increasing temperatures. However, the conductivity of SPI was water-dependent, which made conductivity very low, even at high temperatures and under non-humidified conditions [19]. To improve the conductivity of PEMs, we doped SPIs with a PIL [VIm][OTf]. As shown in our previous studies [13,14], the conductivity of PEMs increased substantially. Conductivities of composite membranes in anhydrous environment depended on temperature, ionic liquid concentration in the membrane, the type of polymer matrix, and the possible interactions between conducting ILs and polymers [19]. PIL [VIm][OTf] has a vinyl group attached to an imidazolium ring and a lower melting point (64.3 °C), making it less stable at high temperatures, but leading to better ionomer–PIL interactions, which plays a major role in determining the conductivity of IL-doped SPI PEMs [28]. Higher amounts of ionic liquid in composite membranes were expected to further enhance ionic conductivity, but were usually accompanied by reduced mechanical strength and dimensional stability at elevated temperatures [13]. Mechanical properties exhibited a similar trend to the thermal properties. Tensile strength decreased and strain increased with increasing amount of *p*BABTS or ionic liquid in SPI and SPI/PIL composite films. The prepared SPI/PIL composite materials had a higher elongation at break but had lower tensile strength than pristine SPI. For SPI2nS/V₄₀, this PEM had an elongation at break of 33.7%, which increased from 10.2% for SPI2nS. However, the tensile stress decreased from 33.1 MPa for SPI2nS to 4.6 MPa for SPI2nS/V₄₀. Therefore, to balance the conductivity and properties of PEM, we chose composite membranes with 40% PIL composition in most of our studies.

3.5.1. Effect of Sulfonated Diamine on PEM Conductivity

The membranes comprised of a polymer with sulfonic acid groups exhibited higher ionic conductivities than those comprised of neutral polymers [29]. As expected, the compounds with a higher content of sulfonic acid groups in the molecular structure had higher IEC values. IEC values increased with *p*BABTS content in SPIs. IEC_(theory) started from 1.98 for SPI1nS (contained 25% *p*BABTS) and increased to 2.64 for SPI3nS (35% *p*BABTS). IEC_(exp) had similar trends. Experimental IECs (by titration) agreed well with those calculated from the feed molar ratios (Table 1). We investigated the conductivities of SPI/PIL prepared from a sulfonated diamine ODADS in recent studies [13,14]. By using the same polymer system (BAPP diamine and ODPA dianhydride) with the exception of a different and novel sulfonated diamine (*p*BABTS), SPI/PIL membranes prepared from *p*BABTS offered higher IEC values and as much as twice the conductivities as those membranes made by ODADS as depicted in Figure 5. SPIa, SPIb, and SPIc referred to SPIs synthesized by 25%, 30%, and 35% ODADS, respectively, as defined previously [13]. SPI3pO/V₄₀ had a conductivity of 2.76 mS/cm versus only 1.42 mS/cm with SPIc/V₄₀ at 110 °C and in an anhydrous or non-humid condition.

3.5.2. Effect of Various Diamines in SPI on PEM Conductivity

As we discussed in our previous reports, sulfonated diamine improved the conductivity of SPIs, but the mechanical and thermal properties could be reduced [13,14]. To enhance the physical properties of SPIs, other diamines can be utilized in polymerization. Three diamines were investigated: BAPP, BAPN,

and 9FDA. The experimental results showed in Figure 6a demonstrated that SPI/PIL PEMs fabricated from 9FDA had the highest conductivity among three diamines, followed by BAPN then BAPP. A SPI/PIL composite PEM was prepared using 9FDA as the diamine and ODPAs as the dianhydride, and doped with 40 wt% [VIm][OTf]. A conductivity of 8.35 mS/cm was obtained at 120 °C in an anhydrous condition. This can be attributed to the chemical structure variation of these diamines, as 9FDA has a bulky lateral fluorene group that forced polymer chains apart and produced large interchain spacing. Within this spacing, water molecules could be confined and would prevent evaporation at high temperatures, resulting in higher conductivities [30].

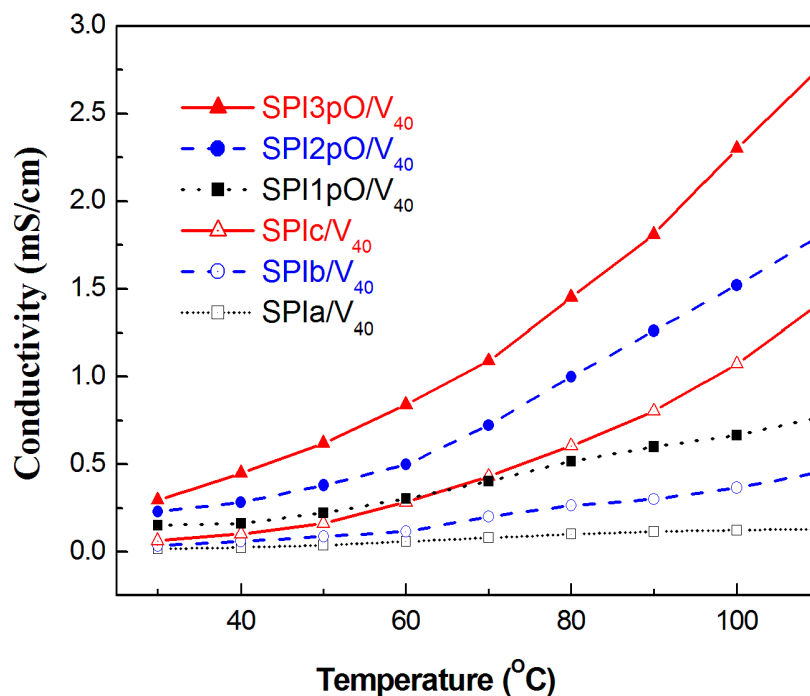
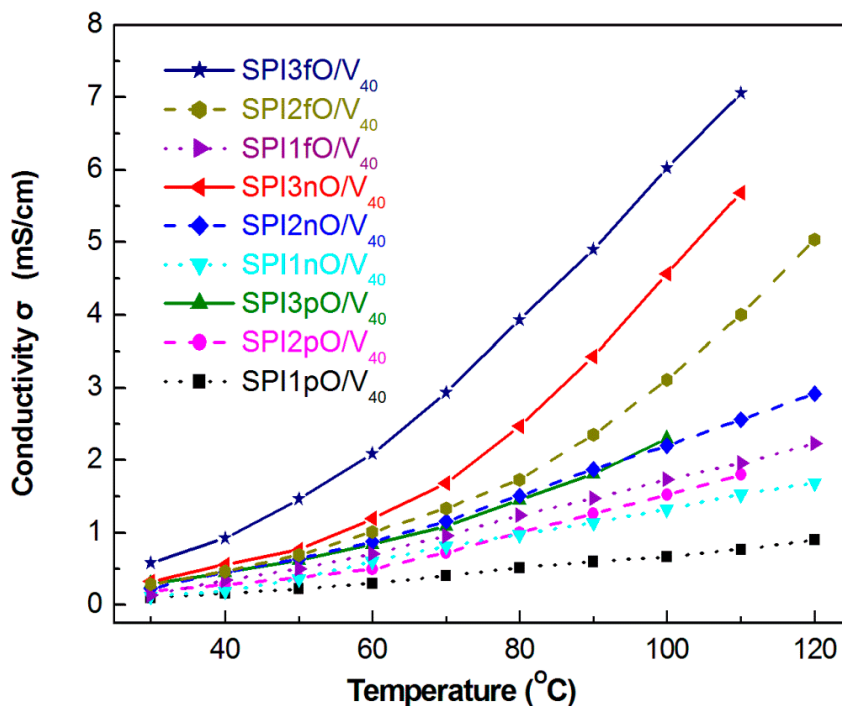


Figure 5. Temperature dependence of conductivity of SPI/PIL composite membranes prepared from different sulfonated diamines (*p*BABTS vs. ODADS).

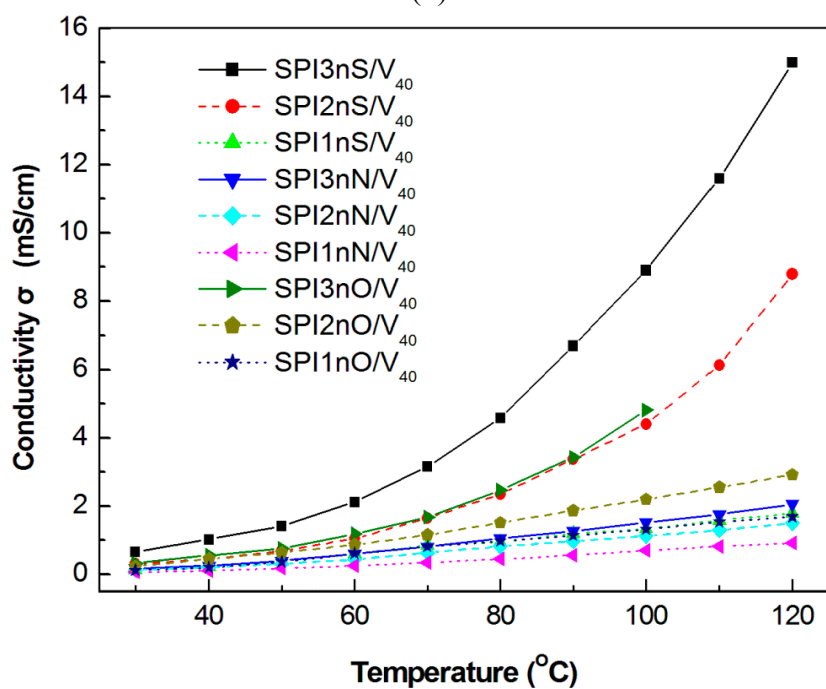
3.5.3. Effect of Various Dianhydrides in SPI on PEM Conductivity

Recently, we studied SPIs based on ODADS sulfonated diamine and found that the conductivity of SPI/PIL PEM prepared from dianhydride DSDA was much higher than that made from 4,4'-bisphenol A dianhydride (BPADA) and higher than that from ODPAs [14]. In this study, we investigated the effect of various dianhydrides on the conductivity of SPI/PIL prepared from *p*BABTS. Three dianhydrides (ODPA, NTDA, and DSDA) were studied. The measured conductivities showed in Figure 6b illustrated that SPI/PIL PEMs prepared from DSDA had the highest conductivity among three dianhydrides, followed by ODPAs and NTDA. A SPI/PIL composite PEM (SPI3nS/V₄₀) was prepared using BAPN as the diamine and DSDA as the dianhydride, and doped with 40 wt % [VIm][OTf]. A conductivity of 14.6 mS/cm was obtained at 120 °C under anhydrous or non-humid conditions. This can be accredited to the chemical structure variation of these dianhydrides, as DSDA has a sulfonyl group that enhances conductivity, though SPIs containing NTDA have higher IEC values.

This illustrated the important role that the chemical structure of dianhydride plays in the conductivity of PEMs.



(a)



(b)

Figure 6. Temperature dependence of conductivity of SPI/PIL composite membranes prepared from (a) ODPA dianhydride and various diamines; and (b) BAPN diamine and various dianhydrides.

3.5.4. Conductivity Comparison with Nafion 117

Based on the above results, diamine 9FDA and dianhydride DSDA were the best among the three diamines and dianhydrides under study, respectively. We fabricated novel PEMs by utilizing *p*BABTS sulfonated diamine, 9FDA, and DSDA to synthesize SPIs and doped with PIL [VIm][OTf]. It was expected that SPI3fS/V₄₀ would have the highest ionic conductivity among all SPI/IL composite membranes studied. However, the glass transition temperature (T_g) of SPI3fS/V₄₀ was only around 100 °C. Higher operating temperatures for PEMFC are desirable because catalyst poisoning by absorbed CO can be reduced and hydrogen with less purity can be used. In addition, the kinetics of the chemical reactions could be accelerated by increasing the temperature. Therefore, we only presented the conductivities of SPI2fS and SPI1fS doped with PIL 40% (SPI2fS/V₄₀ and SPI1fS/V₄₀) and 30% (SPI2fS/V₃₀ and SPI1fS/V₃₀). Figure 7 shows the Arrhenius plot for the temperature-dependent conductivities of these novel SPIs doped with PIL at ambient environment (60%–70% humidity). The conductivities of Nafion 117 were also included as a reference membrane for comparison. As depicted in Figure 7, the proton conductivities of Nafion 117 under ambient condition were less than those measured from SPI/PIL membranes prepared with *p*BABTS/9FDA/DSDA novel polymer. SPI2fS/V₄₀ PEM had a proton conductivity of 16.3 mS/cm at 120 °C and will be used in fuel cell tests.

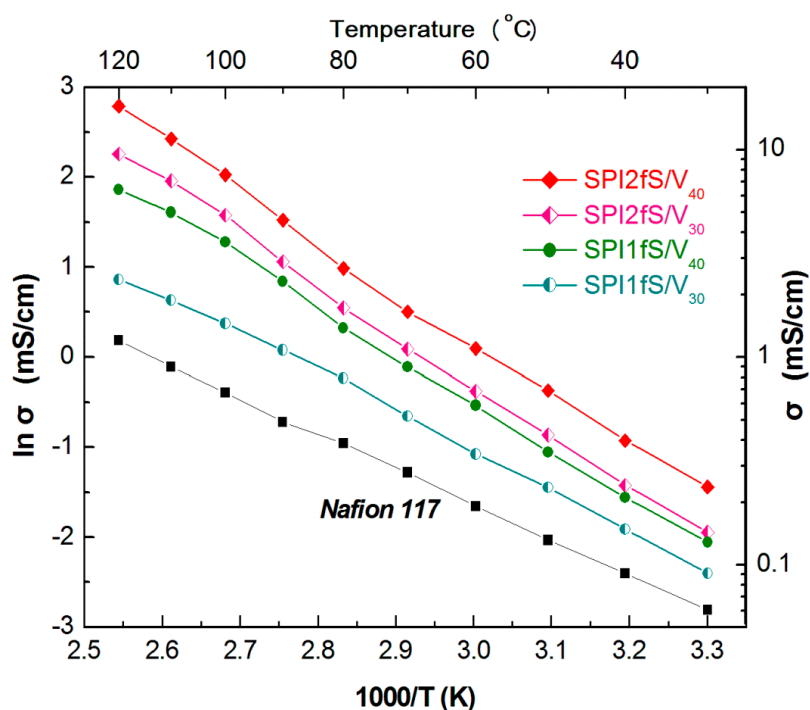


Figure 7. Arrhenius plot for the temperature-dependent conductivities of Nafion 117 and SPIs doped with PIL 30% and 40% under ambient conditions.

3.6. Morphology Studies

The properties of membranes are closely related to their microstructures. Sekhon *et al.* concluded that both the hydrophilicity of impregnated ionic liquids and the structure of the polymer matrix affected the morphology of formed membranes, which was directly related to the ionic conductivity of membranes [11]. The morphologies of SPIs and SPL/PIL composite membranes were analyzed using

a scanning electron microscope (SEM) under ambient conditions (Figure 8). The SEM image of SPIs showed a flat topography (same as Figure 5a in our previous report [14]), while the images of SPI/PIL show a homogeneous, PIL dispersed morphology (Figure 8a). The cross-sectional view of SPI/PIL films showed a dense membrane. However, if we immersed a SPI/PIL membrane in water for 24 h, it formed a membrane with nanosize pores (Figure 8b). The morphology of the membrane containing hydrophilic [OTf] showed better connectivity than the membrane containing a hydrophobic IL, resulting in higher conductivity [2]. This suggests that morphology plays an important role in IL-based PEM design. To confirm the existence of ionic liquids in SPI/PIL PEMs, EDS was utilized to quantify several elements, as shown in Figure 9a. The element Pt may have come from the sample holder where PEM films were placed. The element-mapping of fluorine (F, the unique element in PIL of SPI/PIL PEMs) in a SPI2fS/V₄₀ PEM is illustrated in Figure 9b. The bright spots corresponding to the F element were found to be homogeneously dispersed in the black background (*i.e.*, polymer matrix). All this evidence demonstrates that ionic liquids were included inside the SPI polymer matrix.

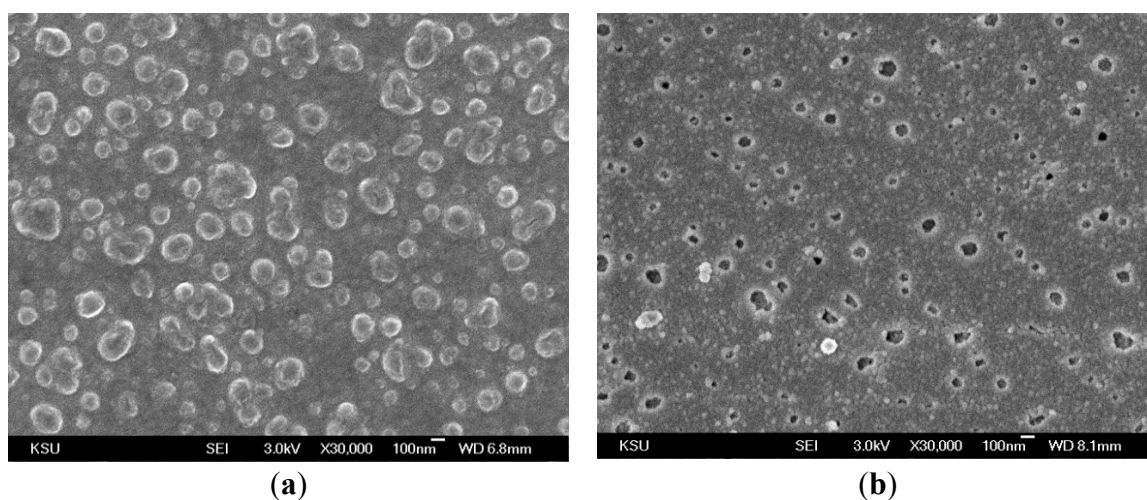


Figure 8. SEM morphology of SPI/PIL composite membranes. (a) SPI2fS/V₄₀ (30,000 magnification) and (b) SPI2fS/V₄₀ after water immersion.

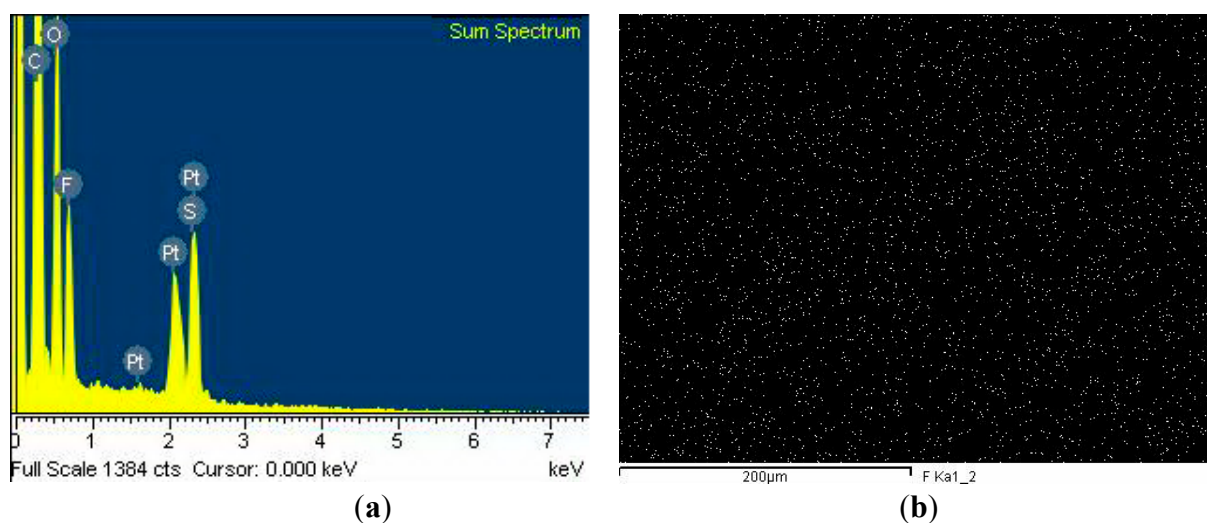


Figure 9. (a) EDS spectrum and (b) F mapping of SPI2fS/V₄₀ PEM.

4. Conclusions

Novel SPI/PIL composite membranes were prepared and characterized as potential PEM materials with improved proton conductivity. SPIs were synthesized from a novel sulfonated diamine, *p*BABTS, and various diamines (BAPP, BAPN, or 9FDA), and an aromatic dianhydride (ODPA, NTDA, or DSDA). SPI2fS/V₄₀ PEM had a high proton conductivity of 16.3 mS/cm at 120 °C in anhydrous conditions and outperformed SPI/PIL composite PEM using sulfonated diamine ODADS and 50 wt% [VIm][OTf] with a conductivity of 6 mS/cm. *p*BABTS offered better conductivity than ODADS, due to having more sulfonated groups that provide increased conductivity. 9FDA exhibited the highest conductivity among the three investigated diamines, which can be accounted for by the chemical structure of 9FDA, which has bulky lateral fluorene groups. The bulky groups could produce large interchain spacing that would prevent water molecules from evaporating at high temperatures, resulting in higher conductivities. Dianhydride DSDA showed the best conductivity, which can be related to the chemical structure of DSDA, which has a sulfonyl group to provide better conductivity. Protic IL [VIm][OTf] substantially increased the conductivity of PEMs. The obtained composite membranes exhibited good thermal stability ($T_d > 300$ °C) and high ionic conductivity under anhydrous or non-humid conditions. The novel SPI/PIL composite membrane can be used as a prospective PEM candidate for intermediate temperature fuel cell applications.

Acknowledgments

Financial support from the Ministry of Science and Technology of Taiwan (MOST 103-2221-E-168-033) is gratefully acknowledged.

Author Contributions

Bor-Kuan Chen wrote the paper, Jhong-Ming Wong, Yu-Ming Chang and Hsu-Feng Lee performed polymer syntheses, characterizations, and TGA, DSC experiments, and Tzi-Yi Wu and Wen-Yao Huang provided the guidance of experiments. Antonia F. Chen edited the entire manuscript.

Conflicts of Interest

The authors declare no conflict of interest.

References

1. Chandan, A.; Hattenberger, M.; El-kharouf, A.; Du, S.; Dhir, A.; Self, V.; Pollet, B.G.; Ingram, A.; Bujalski, W. High temperature (HT) polymer electrolyte membrane fuel cells (PEMFC)—A review. *J. Power Sources* **2013**, *231*, 264–278.
2. Ye, Y.S.; Rick, J.; Hwang, B.J. Water soluble polymers as proton exchange membranes for fuel cells. *Polymers* **2012**, *4*, 913–963.
3. Diaz, M.; Ortiz, A.; Ortiz, I. Progress in the use of ionic liquids as electrolyte membranes in fuel cells. *J. Membrane Sci.* **2014**, *469*, 379–396.

4. Park, C.H.; Lee, C.H.; Guiver, M.D.; Lee, Y.M. Sulfonated hydrocarbon membranes for medium-temperature and low-humidity proton exchange membrane fuel cells (PEMFCs). *Prog. Polym. Sci.* **2011**, *36*, 1443–1498.
5. Marestin, C.; Gebel, G.; Diat, O.; Mercier, R. Sulfonated Polyimides. *Adv. Polym. Sci.* **2008**, *216*, 185–258.
6. Yan, J.; Liu, C.; Wang, Z.; Xing, W.; Ding, M. Water resistant sulfonated polyimides based on 4,4'-binaphthyl-1,1',8,8'-tetracarboxylic dianhydride (BNTDA) for proton exchange membranes. *Polymer* **2007**, *48*, 6210–6214.
7. Chen, B.K.; Tsay, S.Y.; Chiu, T.M. Synthesis and characterization of polyimide/silica hybrid nanocomposites. *J. Appl. Polym. Sci.* **2004**, *94*, 382–393.
8. Ye, Y.S.; Rick, J.; Hwang, B.J. Ionic liquid polymer electrolytes. *J. Mater. Chem. A* **2013**, *1*, 2719–2743.
9. Luo, J.; Conrad, O.; Vankelecom, I.F.J. Imidazolium methanesulfonate as a high temperature proton conductor. *J. Mater. Chem. A* **2013**, *1*, 2238–2247.
10. Doyle, M.; Choi, S.K.; Proulx, G. High-temperature proton conducting membranes based on perfluorinated ionomer membrane-ionic liquid composites. *J. Electrochem. Soc.* **2000**, *147*, 34–37.
11. Sekhon, S.S.; Park, J.S.; Cho, E.K.; Yoon, Y.G.; Kim, C.S.; Lee, W.Y. Studies of high temperature proton conducting membranes containing hydrophilic/hydrophobic ionic liquids. *Macromolecules* **2009**, *42*, 2054–2062.
12. Lee, S.Y.; Yasuda, T.; Watanabe, M. Fabrication of protic ionic liquid/sulfonated polyimide composite membranes for non-humidified fuel cells. *J. Power Sources* **2010**, *195*, 5909–5914.
13. Chen, B.K.; Wu, T.Y.; Kuo, C.W.; Peng, Y.C.; Shih, I.C.; Hao, L.; Sun, I.W. 4,4'-Oxydianiline (ODA) containing sulfonated polyimide/protic ionic liquid composite membranes for anhydrous proton conduction. *Int. J. Hydrog. Energy* **2013**, *38*, 11321–11330.
14. Chen, B.K.; Wong, J.M.; Wu, T.Y.; Chen, L.C.; Shih, I.C. Improving the conductivity of sulfonated polyimides as proton exchange membranes by doping of a protic ionic liquid. *Polymers* **2014**, *6*, 2720–2736.
15. Wu, T.Y.; Sun, I.W.; Gung, S.T.; Chen, B.K.; Wang, H.P.; Su, S.G. High conductivity and low viscosity Brønsted acidic ionic liquids with oligomeric anions. *J. Taiwan Inst. Chem. Eng.* **2011**, *42*, 874–881.
16. Wu, T.Y.; Chen, B.K.; Hao, L.; Lin, K.F.; Sun, I.W. Thermophysical properties of a room temperature ionic liquid (1-methyl-3-pentyl-imidazolium hexafluorophosphate) with poly(ethylene glycol). *J. Taiwan Inst. Chem. Eng.* **2011**, *42*, 914–921.
17. Luo, J.; Hu, J.; Saak, W.; Beckhaus, R.; Wittstock, G.; Vankelecom, I.F.J.; Agerta, C.; Conrad, O. Protic ionic liquid and ionic melts prepared from methanesulfonic acid and 1*H*-1,2,4-triazole as high temperature PEMFC electrolytes. *J. Mater. Chem.* **2011**, *21*, 10426–10436.
18. Pibiri, I.; Pace, A.; Buscemi, S.; Causin, V.; Rastrelli, F.; Saielli, G. Oxadiazolyl-pyridines and perfluoroalkyl-carboxylic acids as building blocks for protic ionic liquids: crossing the thin line between ionic and hydrogen bonded materials. *Phys. Chem. Chem. Phys.* **2012**, *14*, 14306–14314.
19. Deligöz, H.; Yılmazoğlu, M. Development of a new highly conductive and thermomechanically stable complex membrane based on sulfonated polyimide/ionic liquid for high temperature anhydrous fuel cells. *J. Power Sources* **2011**, *196*, 3496–3502.

20. Schauer, J.; Sikora, A.; Pliškova, M.; Mališ, J.; Mazur, P.; Paidar, M.; Bouzek, K. Ion-conductive polymer membranes containing 1-butyl-3-methylimidazolium trifluoromethanesulfonate and 1-ethylimidazolium trifluoromethanesulfonate, *J. Membrane Sci.* **2011**, *367*, 332–339.
21. Van de Ven, E.; Chairuna, A.; Merle, G.; Benito, S.P.; Borneman, Z.; Nijmeijer, K. Ionic liquid doped polybenzimidazole membranes for high temperature proton exchange membrane fuel cell applications. *J. Power Sources* **2013**, *222*, 202–209.
22. Ye, Y.S.; Tseng, C.Y.; Shen, W.C.; Wang, J.S.; Chen, K.J.; Cheng, M.Y.; Rick, J.; Huang, Y.J.; Chang, F.C.; Hwang, B.J. A new graphene-modified protic ionic liquid-based composite membrane for solid polymer electrolytes. *J. Mater. Chem.* **2011**, *21*, 10448–10453.
23. Leu, T.S.; Wang, C.S. Synthesis and properties of copolyimides containing naphthalene group. *Polymer* **2002**, *43*, 7069–7074.
24. Gao, Y.; Robertson, G.P.; Guiver, M.D. Ean, X.G.; Mikhailenko, S.D.; Wang, K.P.; Kaliaguine, S. Sulfonation of poly(phthalazinones) with fuming sulfuric acid mixtures for proton exchange membrane materials. *J. Membr. Sci.* **2003**, *227*, 39–50.
25. Luo, J.; Tan, T.V.; Conrad, O.; Vankelecom, I.F.J. 1*H*-1,2,4-Triazole as solvent for imidazolium methanesulfonate. *Phys. Chem. Chem. Phys.* **2012**, *14*, 11441–11447.
26. Bai, H.; Ho, W.S.W. New poly(ethylene oxide) soft segment-containing sulfonated polyimide copolymers for high temperature proton-exchange membrane fuel cells. *J. Membr. Sci.* **2008**, *313*, 75–85.
27. Hirao, M.; Ito, K.; Ohno, H. Preparation and polymerization of new organic molten salts; *N*-alkylimidazolium salt derivatives. *Electrochim. Acta* **2000**, *45*, 1291–1294.
28. Ohno, H. *Electrochemical Aspects of Ionic Liquids*; Wiley Interscience: Hoboken, NJ, USA, 2005.
29. Higashihara, T.; Matsumoto, K.; Ueda, M. Sulfonated aromatic hydrocarbon polymers as proton exchange membranes for fuel cells. *Polymer* **2009**, *50*, 5341–5357.
30. Ye, X.; Bai, H.; Ho, W.S. Synthesis and characterization of new sulfonated polyimides as proton-exchange membranes for fuel cells. *J. membrane Sci.* **2006**, *279*, 570–577.